

## Article

# Minimizing Risk of Failure from Ceramic-on-Ceramic Total Hip Prosthesis by Selecting Ceramic Materials Based on Tresca Stress

Muhammad Imam Ammarullah <sup>1,2,3,\*</sup> , Gatot Santoso <sup>1,2</sup> , S. Sugiharto <sup>1,2</sup> , Toto Supriyono <sup>1,2</sup>,  
Dwi Basuki Wibowo <sup>4</sup>, Ojo Kurdi <sup>4</sup>, Mohammad Tauviquirrahman <sup>4</sup> and J. Jamari <sup>3,4</sup> 

<sup>1</sup> Department of Mechanical Engineering, Faculty of Engineering, Pasundan University, Bandung 40153, West Java, Indonesia

<sup>2</sup> Biomechanics and Biomedics Engineering Research Centre, Faculty of Engineering, Pasundan University, Bandung 40153, West Java, Indonesia

<sup>3</sup> Undip Biomechanics Engineering & Research Centre (UBM-ERC), Diponegoro University, Semarang 50275, Central Java, Indonesia

<sup>4</sup> Department of Mechanical Engineering, Faculty of Engineering, Diponegoro University, Semarang 50275, Central Java, Indonesia

\* Correspondence: imamammarullah@gmail.com; Tel.: +62-895-3359-22435



**Citation:** Ammarullah, M.I.; Santoso, G.; Sugiharto, S.; Supriyono, T.; Wibowo, D.B.; Kurdi, O.; Tauviquirrahman, M.; Jamari, J. Minimizing Risk of Failure from Ceramic-on-Ceramic Total Hip Prosthesis by Selecting Ceramic Materials Based on Tresca Stress. *Sustainability* **2022**, *14*, 13413. <https://doi.org/10.3390/su142013413>

Academic Editors: Posinasetti Nageswara Rao, Prasad KDV Yarlagadda and Immanuel Edinbarough

Received: 3 August 2022

Accepted: 9 October 2022

Published: 18 October 2022

**Publisher's Note:** MDPI stays neutral with regard to jurisdictional claims in published maps and institutional affiliations.



**Copyright:** © 2022 by the authors. Licensee MDPI, Basel, Switzerland. This article is an open access article distributed under the terms and conditions of the Creative Commons Attribution (CC BY) license (<https://creativecommons.org/licenses/by/4.0/>).

**Abstract:** The choice of ceramic-on-ceramic coupling in total hip prosthesis has advantages over couplings with other combinations of materials that use polyethylene and metal materials in terms of high hardness, scratch resistance, low wear rate, and increased lubrication performance. To reduce the risk of primary postoperative failure, the selection of ceramic materials for ceramic-on-ceramic coupling is a strategic step that needs to be taken. The current study aims to analyze ceramic-on-ceramic coupling with commonly used ceramic materials, namely zirconium dioxide ( $ZrO_2$ ), silicon nitride ( $Si_3N_4$ ), and aluminium oxide ( $Al_2O_3$ ), according to Tresca failure criterion for the investigation of the stress distribution. A two-dimensional axisymmetric finite element-based computational model has been used to evaluate the Tresca stress on ceramic-on-ceramic coupling under gait cycle. The results show that the use of  $ZrO_2$ -on- $ZrO_2$  couplings can reduce Tresca stress by about 17.34% and 27.23% for  $Si_3N_4$ -on- $Si_3N_4$  and  $Al_2O_3$ -on- $Al_2O_3$  couplings, respectively.

**Keywords:** aluminium oxide; ceramic-on-ceramic; gait cycle; total hip prosthesis; Tresca stress; silicon nitride; zirconium dioxide

## 1. Introduction

Restoring the condition of the inflamed hip joint through surgery with total hip replacement is a surgical intervention that is highly effective today [1–3]. However, active implant users who have a longer life expectancy are still found to undergo revision surgery due to various causes of implant failure [4]. One of the main components in a total hip replacement that needs to be evaluated to minimize implant failure is a coupling that provides articulation for the user to accommodate the many activities that implant users perform. In this case, material coupling selection has a strategic role in improving the performance of total hip replacement [5].

The use of conventional polyethylene as a coupling material with a hard-on-soft combination, such as metal-on-polyethylene and ceramic-on-polyethylene, has begun to be limited due to the high number of wear cases that affect long-term performance [6]. Additionally, polyethylene wear particles give a negative body response to implant users [7]. Although the use of metal-on-metal couplings was once an option, the relatively high number of failure cases found compared to other material combinations made this coupling less desirable. In addition, the issue of metal ions being harmful to the user's body from metal wear particles of metal-on-metal couplings is also a reason for the lack of interest in these couplings [8,9].

Therefore, ceramic-on-ceramic couplings have become the surgeon's choice because of concerns about the dangers of using other couplings [10]. The main advantages presented by using ceramic-on-ceramic coupling are their high hardness [11], scratch resistance [12], low wear rate [13], and increased lubrication performance [14]. In terms of wear particles, ceramic materials produce less when compared to polyethylene or metallic materials [15]. Unfortunately, the use of ceramic-on-ceramic couplings is prone to fracture, due to high-intensity activities which result in the need for revision operations [16]. The selection of ceramic materials for ceramic-on-ceramic couplings is important in minimizing revision operations that are harmful to the user. Several ceramic materials available and commonly used in ceramic-on-ceramic total hip replacement couplings are zirconium dioxide ( $ZrO_2$ ) [17], silicon nitride ( $Si_3N_4$ ) [18], and aluminium oxide ( $Al_2O_3$ ) [19].

The evaluation of ceramic materials for ceramic-on-ceramic total hip prosthesis is essential to confirm long-term implant durability with stress analysis. Von Mises stress analysis has been widely adopted in the literature for medical implant analysis, as done by Carreiras et al. [20] and Fernandes et al. [21], but implant failure cases are still reported today that need more in-depth stress study since it is related to implant failure, and to ensure safer prosthesis for the patient. A better option is offered by analyzing the failure using Tresca stress because it is safer than von Mises, because the safety area of Tresca stress based on Tresca failure theory is lower when compared to von Mises stress area based on von Mises failure theory [22]. Tresca stress studies on total hip prosthesis couplings were previously carried out by Ammarullah et al. for metal-on-ultra high molecular weight polyethylene (UHMWPE) [23,24] and metal-on-metal [25]. However, Tresca stress studies to evaluate different ceramic materials for ceramic-on-ceramic coupling have not been performed.

The current study aims to analyze ceramic-on-ceramic couplings with three different types of ceramic materials using Tresca stresses. The finite element approach is used to accommodate computational simulation investigations. Loading is simulated by adopting a gait cycle that reflects the actual condition of the implant user.

## 2. Materials and Methods

### 2.1. Geometry and Material Configuration

The geometry of coupling in the current study for the components of the femoral head and acetabular cup, referring to the work of Jamari et al. [26] and which are commonly used in total hip replacement, are shown in Table 1.

**Table 1.** Coupling geometry of total hip replacement [26].

Parameter	Size (mm)
Femoral head diameter	28
Radial clearance	0.05
Acetabular cup thickness	5

Material properties of three different ceramic materials in the present study were adopted from previously published works:  $ZrO_2$  from Jin et al. [27],  $Si_3N_4$  from Dubiel et al. [28], and  $Al_2O_3$  from Aherwar et al. [29]. These are shown in Table 2. Material assumption for all simulated ceramic materials is set to be homogeneous, isotropic, and linear elastic, with a consideration for their Young modulus and Poisson ratio regarding their mechanical properties. The assumptions refer to previous studies conducted by Uddin and Zhang [30], Jagatia and Jin [31], Shankar [32], and Cilingir et al. [33].

The coefficient of friction is obtained from a hip joint simulator or a pin-on-disc test [30,34,35]. In the current computational simulation, the values for the coefficient of friction are adopted from published works:  $ZrO_2$ -on- $ZrO_2$  from Ruggiero et al. [36],  $Si_3N_4$ -on- $Si_3N_4$  from Shankar and Nithyaprakash [37], and  $Al_2O_3$ -on- $Al_2O_3$  from Shankar et al. [32]. These are shown in Table 3.

**Table 2.** Data input of ceramic materials [27–29].

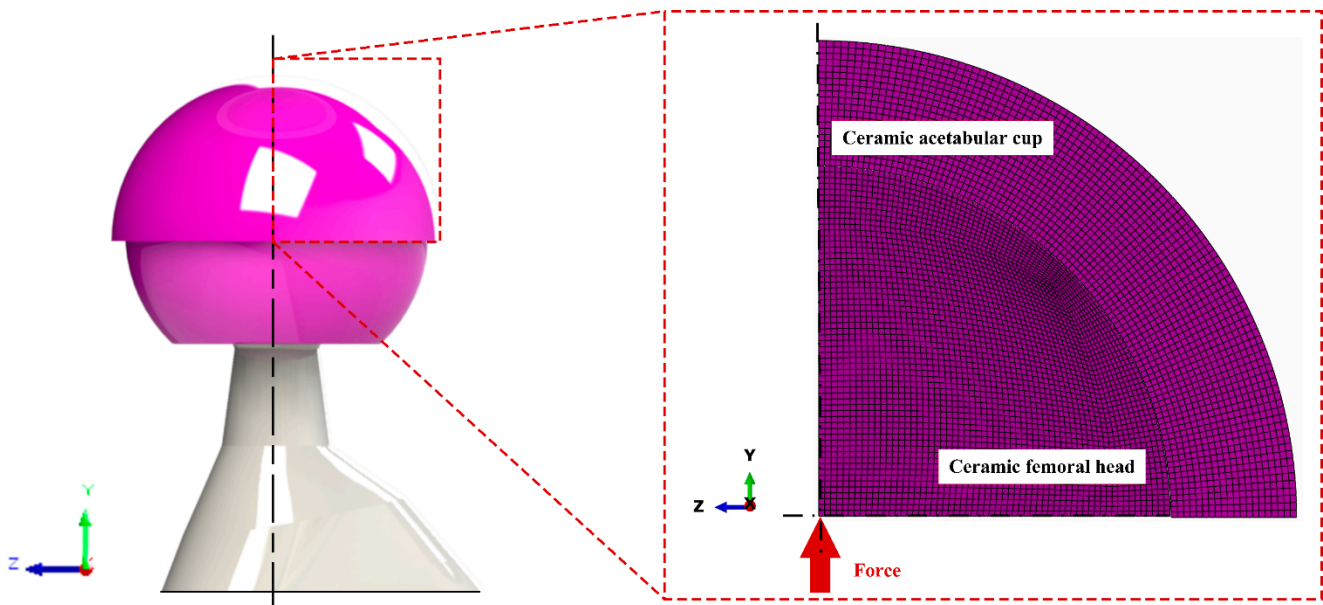
Ceramic Materials	Young's Modulus (GPa)	Poisson's Ratio (-)
ZrO <sub>2</sub>	210	0.26
Si <sub>3</sub> N <sub>4</sub>	300	0.29
Al <sub>2</sub> O <sub>3</sub>	375	0.3

**Table 3.** Coefficient of friction value for various ceramic-on-ceramic couplings [32,36,37].

Ceramic-on-Ceramic Couplings	Coefficient of Friction (-)
ZrO <sub>2</sub> -on-ZrO <sub>2</sub>	0.49
Si <sub>3</sub> N <sub>4</sub> -on-Si <sub>3</sub> N <sub>4</sub>	0.2
Al <sub>2</sub> O <sub>3</sub> -on-Al <sub>2</sub> O <sub>3</sub>	0.1

## 2.2. FE Model

ABAQUS/CAE 6.14-1 has been used in the current study to simulate steady-state Tresca stress from ceramic-on-ceramic couplings using static loading with an implicit analysis. The hip replacement is shown in Figure 1, where the finite element model uses 5500 four-node axisymmetric elements (CAX4) for 2000 CAX4 and 3500 CAX4, respectively, in the ceramic femoral head and ceramic acetabular cup components through the results of the convergence study. The number of nodes in both a ceramic acetabular cup and a ceramic femoral head were 2124 and 3611 nodes, respectively. Tresca stress was evaluated numerically at each integration point.

**Figure 1.** Finite element model of ceramic-on-ceramic coupling.

The computational burden has been lightened by considering only the femoral head and acetabular cup components as the two main components of a ceramic-on-ceramic total hip prosthesis on a two-dimensional axisymmetric model using a ball-in-socket configuration. Present finite element models of ceramic-on-ceramic coupling only consist of a femoral head and an acetabular cup without adopting other components, such as fixation and cortical bone. Previous research by Jagatia and Jin [31] explained that considerations of cement and cortical bone components in contact investigations between a femoral head and an acetabular cup have no significant effect on the computational simulation results. In addition, the adoption of a two-dimensional finite element model is used in the current study. Cilingir et al. [33] explain that the results of computational simulation results

between two-dimensional and three-dimensional are relatively similar. In addition, the influence of synovial fluid and surface roughness during contact is represented by the coefficient of friction, referred to in previous work by Uddin and Zhang [30].

The application of boundary conditions to the ceramic acetabular cup is conducted by fixing the outer surface in all directions, so that it cannot move. This is based on the fact that, in real terms, this component is still attached to the pelvic bone [25]. As for the femoral head, the position between the ceramic femoral head and the ceramic acetabular cup is made concentric, so that no edge loading is possible. The movement of the femoral head is allowed to move in a vertical direction without any permitted rotation, which is only one degree of freedom. Force from the gait cycle is applied to the bottom of the configured ceramic femoral head in a concentrated manner.

### 2.3. Gait Cycle

Finite element investigation for ceramic-on-ceramic coupling is carried out by applying force according to the physiological condition of the human hip joint in the form of gait cycle, which is the most common activity carried out by implant users [38]. The gait cycle used in the current study adopted a previous approach by Jamari et al. [26], shown in Figure 2, in which one cycle is divided into 32 phases, with the seventh phase being the highest base of 2326 N. Referring to the previous study by Ammarullah et al. [39], gait cycle only considers the resultant vertical force with a negligible range of motion for simplification in the application of two-dimensional axisymmetric models.

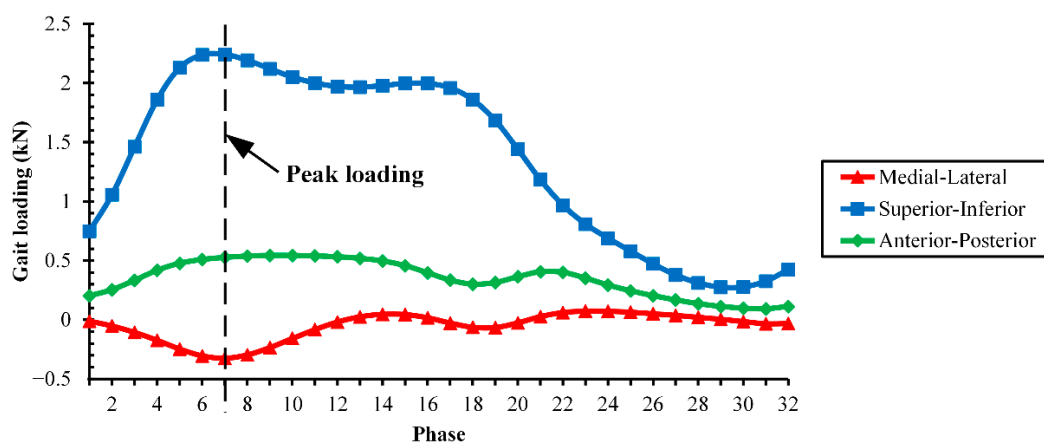


Figure 2. Adopted gait cycle [26].

## 3. Results and Discussion

### 3.1. Convergence Analysis

The selection of the number of elements used in ceramic-on-ceramic coupling was carried out through convergence analysis to investigate the Tresca stress. The convergence study was performed by considering six models with different elements, with an increasing number of elements from one model to another. This determined the number of elements that were sufficient to obtain accurate Tresca stress results, without burdening the computational workload in the ceramic-on-ceramic coupling [9]. Figure 3 shows the comparison of the maximum Tresca stress with the number of elements used for  $\text{Al}_2\text{O}_3$ -on- $\text{Al}_2\text{O}_3$  coupling. The fourth model was chosen when considering the Tresca stress results, whose difference was very small at 1.46 MPa (below 10%) compared to the 6th model with the greatest number of elements. The fourth model uses a total of 5500 elements, with details of 3500 for the ceramic femoral head and 2000 for the ceramic acetabular cup.

### 3.2. Tresca Stress Analysis

Figure 4a presents the maximum Tresca stress for all studied ceramic-on-ceramic couplings for one gait cycle. The variation of the maximum Tresca stress is caused by

different loads received during gait cycles. The highest Tresca stress value was found in the seventh phase on every ceramic-on-ceramic coupling because its phase is the condition of peak loading. The comparison of the highest, average, and lowest Tresca stress can be seen in Figure 4b.

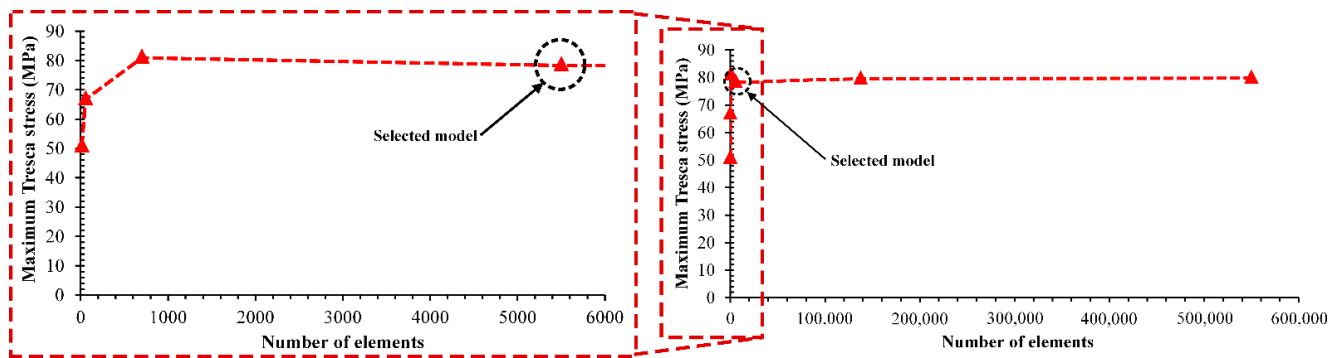


Figure 3. Convergence analysis of  $\text{Al}_2\text{O}_3$ - $\text{Al}_2\text{O}_3$  coupling.

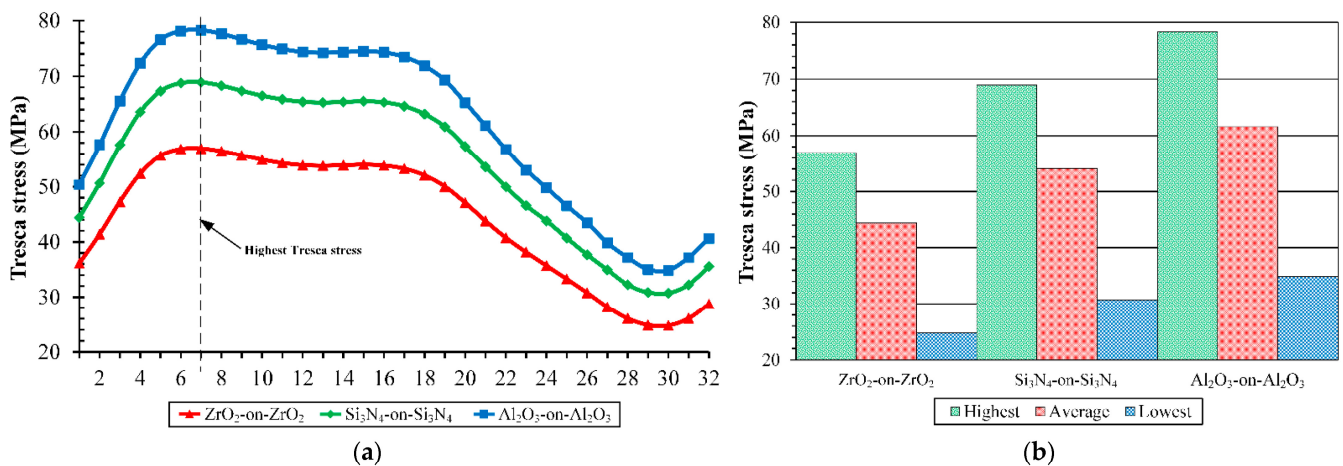


Figure 4. Tresca stress magnitude: (a) maximum during gait cycle and (b) comparison of highest, average, and lowest.

The lowest maximum Tresca stress at the peak loading among ceramic-on-ceramic couplings in the current study was found at  $\text{ZrO}_2$ -on- $\text{ZrO}_2$  of 56.97 MPa. There was an increase of maximum Tresca stress during peak loading found for  $\text{Si}_3\text{N}_4$ -on- $\text{Si}_3\text{N}_4$  of 21.32 MPa and  $\text{Al}_2\text{O}_3$ -on- $\text{Al}_2\text{O}_3$  of about 11.95 MPa compared to  $\text{ZrO}_2$ -on- $\text{ZrO}_2$ . The properties of ceramic material used greatly affected the difference in Tresca stress on ceramic-on-ceramic coupling. With the same magnitude of force applied, ceramic materials that had a higher Young's modulus had a higher Tresca stress value. This caused  $\text{ZrO}_2$ -on- $\text{ZrO}_2$  to have the lowest Tresca stress value, as  $\text{ZrO}_2$  has Young's modulus of 210 GPa, which is the lowest Young's modulus of other ceramic materials in the current work. The maximum Tresca stress values for ceramic-on-ceramic coupling are described in Table 4.

Table 4. Maximum Tresca stress during peak loading.

Ceramic-on-Ceramic Coupling	Maximum Tresca Stress (MPa)
$\text{ZrO}_2$ -on- $\text{ZrO}_2$	56.97
$\text{Si}_3\text{N}_4$ -on- $\text{Si}_3\text{N}_4$	68.92
$\text{Al}_2\text{O}_3$ -on- $\text{Al}_2\text{O}_3$	78.29

Figure 5 shows the contours of Tresca stress distribution performed on ABAQUS [40]. To represent the gait cycle in thirty-two phases, three phases have been chosen to explain changes in the contour distribution referred to in the previous study conducted by Jamari et al. [41]. It is observed that the distribution of Tresca stress is wider and the magnitude is greater along with the higher applied load.

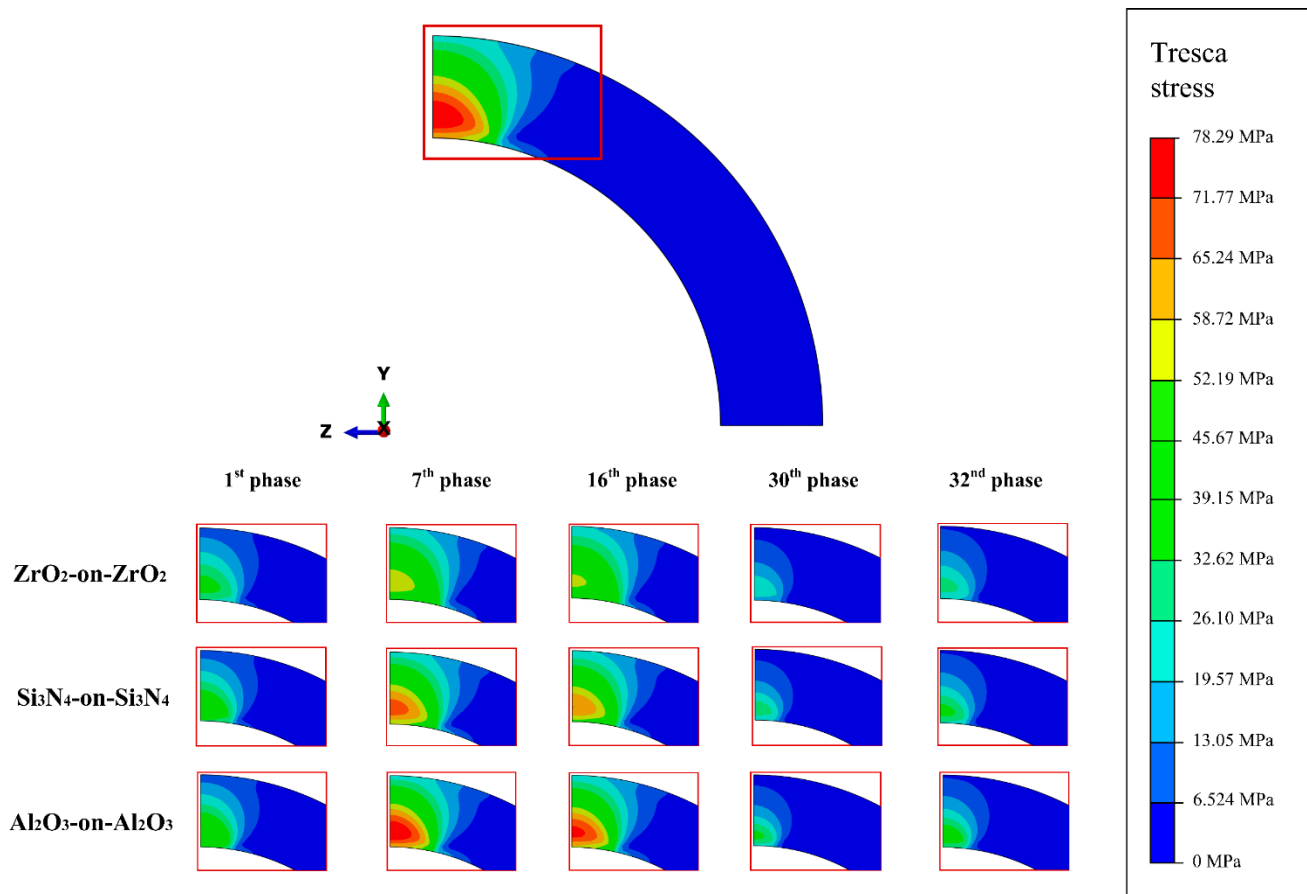


**Figure 5.** The distribution contour of Tresca stress on the thickness of ceramic acetabular cup at selected phases.

To further evaluate the Tresca stress on ceramic-on-ceramic coupling, the relationship between Tresca stress and ceramic acetabular cup thickness is shown during peak loading and selected phases in Figures 6 and 7. The highest Tresca stress is found in the ceramic acetabular cup's thickness in direction y of around 1 cm for all studied ceramic-on-ceramic couplings. It means the highest Tresca stress occurred in the bulk area, not in the contact area, since acting forces caused a change in ceramic acetabular cup volume. The location where the volume of the ceramic acetabular cup decreases more due to acting forces was indicated by the higher Tresca stress magnitude on this area, which occurs in the bulk area of the ceramic acetabular cup. The thickness of the ceramic acetabular cup, which was originally 5 mm, was reduced due to the acting forces when the ceramic-on-ceramic coupling was under gait cycle. In the 7<sup>th</sup> phase (peak loading) of gait cycle, the thickness of the ceramic acetabular cup on the asymmetric axis for ZrO<sub>2</sub>-on-ZrO<sub>2</sub> was 4.99883 mm, Si<sub>3</sub>N<sub>4</sub>-on-Si<sub>3</sub>N<sub>4</sub> was 4.99905 mm, and Al<sub>2</sub>O<sub>3</sub>-on-Al<sub>2</sub>O<sub>3</sub> was 4.99917 mm.

Based on Tresca failure theory, Tresca stress on ceramic-on-ceramic couplings explains the correlation of the probability of future implant failure. Higher Tresca stress means a higher probability of implant failure, and vice versa [23]. From this explanation, ZrO<sub>2</sub>-on-ZrO<sub>2</sub> was the safest coupling, compared to other studied ceramic-on-ceramic couplings.

Based on the current simulation, results of Tresca stress could be used as a reference for developing ceramic-on-ceramic total hip prosthesis to minimize failure in the future. The present study has worked to improve implant performance in ceramic materials selection. In addition, several efforts can be made to improve implant performance, including the evaluation of ceramic-on-ceramic couplings geometry [42], adding dimples on the contact surface [43], surface finish [44], and coating/surfacing applications [45]. Surgical procedures from orthopedic doctors also affect the resistance of the total hip prosthesis after primary surgery [46].

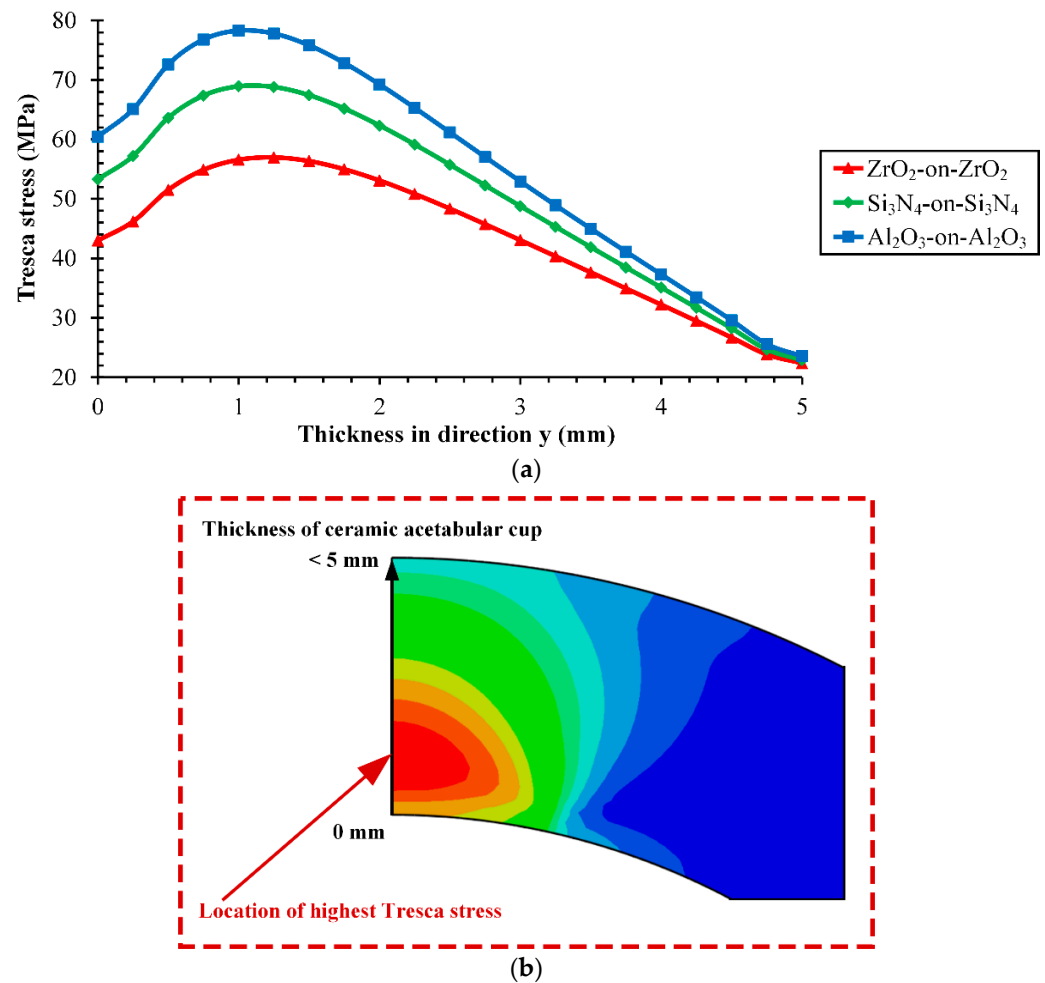


**Figure 6.** (a) Distribution profile of Tresca stress along with ceramic acetabular cup thickness at peak loading and (b) location of highest Tresca stress at ceramic acetabular cup thickness.

A computational simulation-based study on ceramic-on-ceramic coupling has presented implant performance from a biomechanical perspective by looking at Tresca stresses on different ceramic materials. Tresca stress results in the current ceramic-on-ceramic coupling can be one consideration for surgeons in choosing ceramic materials by choosing a ceramic-on-ceramic coupling with the lowest Tresca stress. This means that it has a lower risk of failure among other ceramic materials, according to Tresca's failure theory [22], where it was found that in ZrO<sub>2</sub>-on-ZrO<sub>2</sub> for use in total hip replacement surgery when choosing couplings with the type of ceramic-on-ceramic. However, material selection cannot only be viewed from this perspective. A study is needed from a biomedical perspective so that the selection of materials carried out can provide both better knowledge and clinical relevance [47]. Some biomedical investigations that could be carried out to support the selection of ceramic materials for ceramic-on-ceramic couplings include studies of the

composition of ceramic materials [28] and the possibility of negative body responses due to long-term use [44].

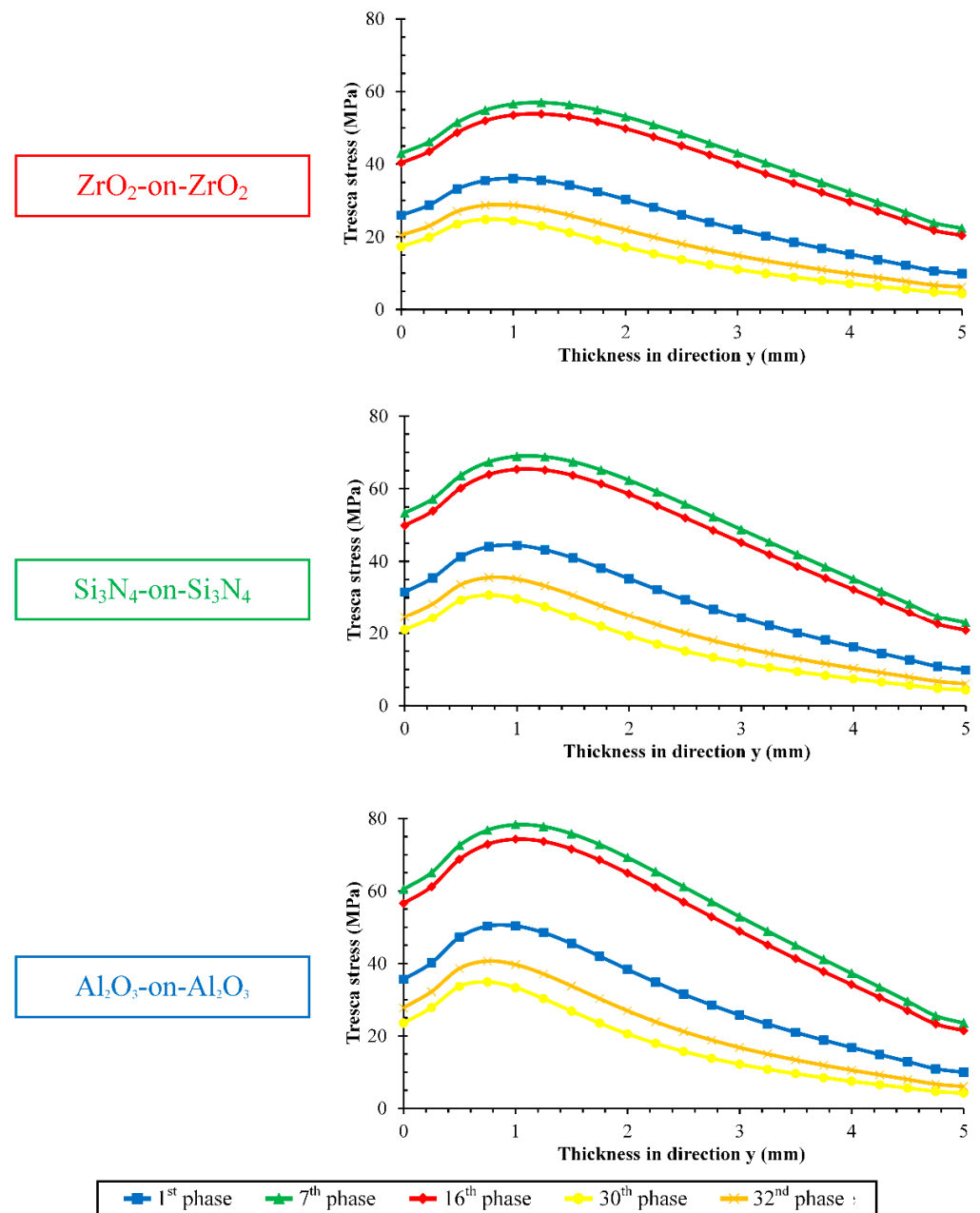


**Figure 7.** Distribution profile of Tresca stress along with ceramic acetabular cup thickness at selected phases.

### 3.3. Comparison of Tresca Stress Results with Similar Published Literature

The maximum Tresca stress at peak loading of gait cycle for the ceramic-on-ceramic coupling in the current study was compared with a similar study with different material combinations, conducted by Ammarullah et al. [23,25]. This is presented in Figure 8. It can be seen that the overall Tresca stress value of the current study is the highest, compared to others. This is because the Young's modulus of ceramic is greater than that of metal and UHMWPE.

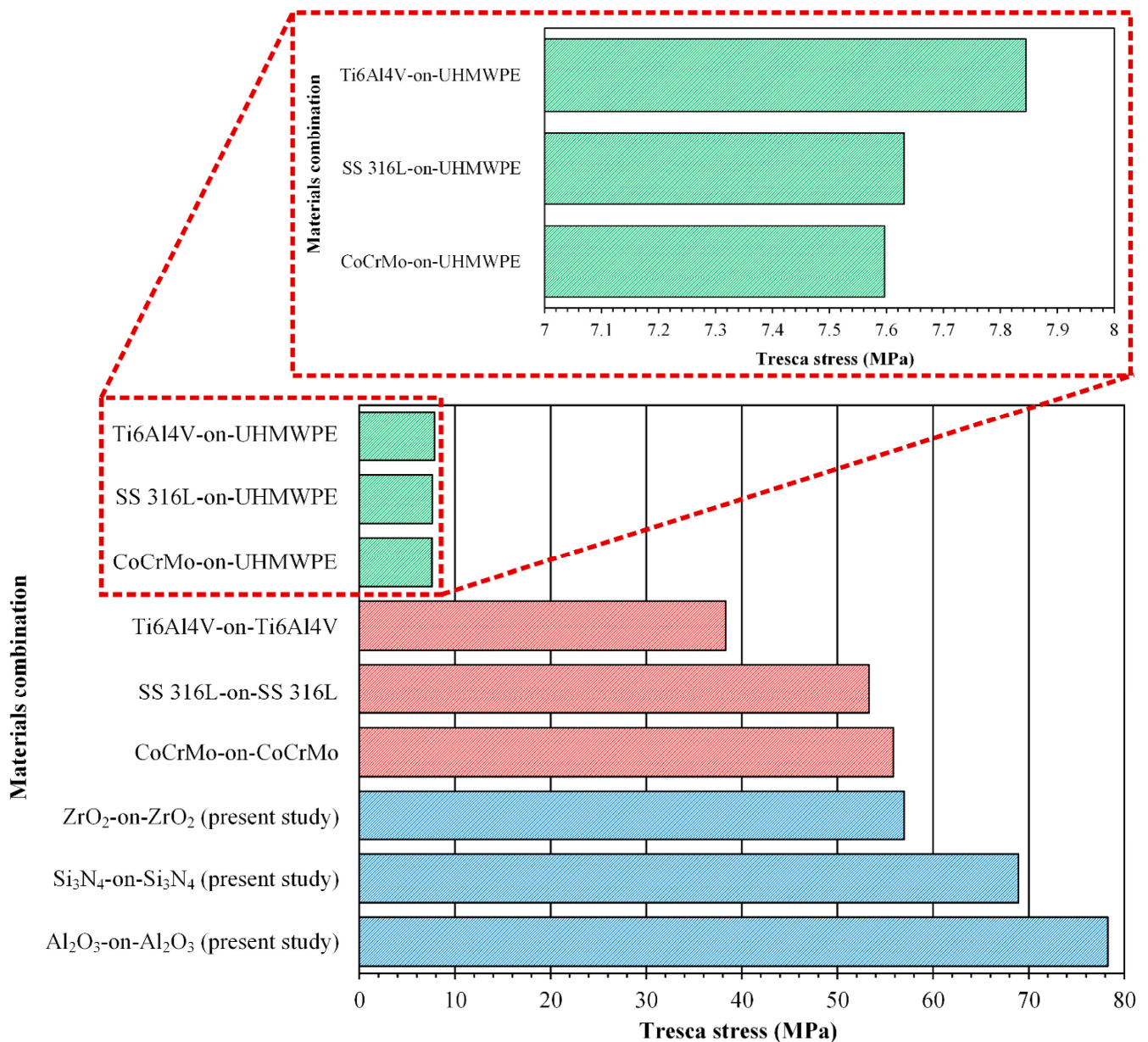


**Figure 8.** Maximum Tresca stress of ceramic-on-ceramic couplings at peak loading of gait cycle from present study compared with metal-on-UHMWPE couplings [23] and metal-on-metal couplings [25].

### 3.4. Limitations

There are several deficiencies in the present investigation that should be mitigated for in further research. The computational simulation model used for ceramic-on-ceramic coupling ignored the presence of synovial fluid [48]. Gait cycle are only described by gait loading, with values varying based on cycles without the application of motion [49]. The finite element model used only considered the femoral head component to represent the femur head, and the acetabular cup to represent the acetabulum, without considering other components, such as fixation and femoral stem for lighter computations [50].

### 4. Conclusions

The prediction of a computational model from ceramic-on-ceramic coupling based on the finite element method to analyze Tresca stress was successfully carried out. In the seventh phase, the highest Tresca stress was found for every ceramic-on-ceramic coupling model, which is the highest gait loading condition. The distribution of Tresca stress

contour on the ceramic acetabular cup component was found to be wider, along with the higher Tresca stress value. The current simulation shows that ZrO<sub>2</sub>-on-ZrO<sub>2</sub> has a lower Tresca stress than Al<sub>2</sub>O<sub>3</sub>-on-Al<sub>2</sub>O<sub>3</sub> and Si<sub>3</sub>N<sub>4</sub>-on-Si<sub>3</sub>N<sub>4</sub> couplings. It demonstrated that the ZrO<sub>2</sub>-on-ZrO<sub>2</sub> coupling had the best performance to reduce the risk of primary postoperative failure than other ceramic-on-ceramic couplings in the current study. To provide clinical relevance to the results of the current study on material selection for ceramic-on-ceramic couplings, research from biomedical perspectives, such as material composition and potential negative body responses, need to be carried out separately from the biomechanical perspective in the form of Tresca stress.

**Author Contributions:** Conceptualization, M.I.A.; methodology, M.I.A.; software, M.I.A.; validation, M.I.A.; formal analysis, M.I.A.; investigation, M.I.A.; resources, M.I.A.; data curation, M.I.A.; writing—original draft preparation, M.I.A.; writing—review and editing, D.B.W., O.K., M.T. and J.J.; visualization, M.I.A.; supervision, D.B.W., O.K., M.T. and J.J.; project administration, G.S., S.S. and T.S.; funding acquisition, G.S., S.S. and T.S. All authors have read and agreed to the published version of the manuscript.

**Funding:** The research was funded by World Class Research UNDIP number 118-23/UN7.6.1/PP/2021.

**Institutional Review Board Statement:** Not applicable.

**Informed Consent Statement:** Not applicable.

**Data Availability Statement:** The data presented in this study are available on request from the corresponding author.

**Acknowledgments:** Thank you to the Ministry of Education, Culture, Research and Technology of the Republic of Indonesia for their assistance and direction to the first author on behalf of Muhammad Imam Ammarullah in the scientific article writing training held in Bandung, 6–11 June 2022.

**Conflicts of Interest:** The authors declare no conflict of interest.

## References

1. Arthritis Research, UK. *Hip Replacement Surgery—Patient Information*, 2011st ed.; Arthritis Research UK: Chesterfield, UK, 2011.
2. Keele University. *A Guide for People Who Have Osteoarthritis*, 2014th ed.; Keele University: Staffordshire, UK, 2014.
3. London Health Sciences Centre. *My Guide to Total Hip Joint Replacement*, 2013rd ed.; London Health Sciences Centre: London, UK, 2013.
4. Ammarullah, M.I.; Afif, I.Y.; Maula, M.I.; Winarni, T.I.; Tauviqirrahman, M.; Bayuseno, A.P.; Basri, H.; Syahrom, A.; Md Saad, A.P.; Jamari. Deformation Analysis of CoCrMo-on-CoCrMo Hip Implant Based on Body Mass Index Using 2D Finite Element Procedure. *J. Phys. Conf. Ser.* **2022**, *2279*, 012004. [[CrossRef](#)]
5. Al Zoubi, N.F.; Tarlochan, F.; Mehboob, H.; Jarrar, F. Design of Titanium Alloy Femoral Stem Cellular Structure for Stress Shielding and Stem Stability: Computational Analysis. *Appl. Sci.* **2022**, *12*, 1548. [[CrossRef](#)]
6. Speranza, A.; Massafra, C.; Pecchia, S.; Di Niccolo, R.; Iorio, R.; Ferretti, A. Metallic versus Non-Metallic Cerclage Cables System in Periprosthetic Hip Fracture Treatment: Single-Institution Experience at a Minimum 1-Year Follow-Up. *J. Clin. Med.* **2022**, *11*, 1608. [[CrossRef](#)] [[PubMed](#)]
7. Shi, R.; Wang, B.; Liu, J.; Yan, Z.; Dong, L. Influence of Cross-Shear and Contact Pressure on Wear Mechanisms of PEEK and CFR-PEEK in Total Hip Joint Replacements. *Lubricants* **2022**, *10*, 78. [[CrossRef](#)]
8. Silva, D.; Arcos, C.; Montero, C.; Guerra, C.; Martínez, C.; Li, X.; Ringuedé, A.; Cassir, M.; Ogle, K.; Guzmán, D.; et al. A Tribological and Ion Released Research of Ti-Materials for Medical Devices. *Materials* **2022**, *15*, 131. [[CrossRef](#)]
9. Ammarullah, M.I.; Santoso, G.; Sugiharto, S.; Supriyono, T.; Kurdi, O.; Tauviqirrahman, M.; Winarni, T.I.; Jamari, J. Tresca Stress Study of CoCrMo-on-CoCrMo Bearings Based on Body Mass Index Using 2D Computational Model. *Jurnal Tribologi.* **2022**, *33*, 31–38.
10. Australian Orthopaedic Association National Joint Replacement Registry. *Annual Report 2020*, 2020th ed.; Australian Orthopaedic Association: Adelaide, Australia, 2020.
11. Barabashko, M.; Ponomarev, A.; Rezvanova, A.; Kuznetsov, V.; Moseenkov, S. Young's Modulus and Vickers Hardness of the Hydroxyapatite Bioceramics with a Small Amount of the Multi-Walled Carbon Nanotubes. *Materials* **2022**, *15*, 5304. [[CrossRef](#)]
12. Bikulčius, G.; Jankauskas, S.; Selskienė, A.; Staišiūnas, L.; Matijošius, T.; Asadauskas, S.J. New Insight into Adherence of Ni-P Electroless Deposited Coatings on AA6061 Alloy through Al<sub>2</sub>O<sub>3</sub> Ceramic. *Coatings* **2022**, *12*, 594. [[CrossRef](#)]
13. Sharma, A.R.; Lee, Y.-H.; Gankhuyag, B.; Chakraborty, C.; Lee, S.-S. Effect of Alumina Particles on the Osteogenic Ability of Osteoblasts. *J. Funct. Biomater.* **2022**, *13*, 105. [[CrossRef](#)]

14. Sadiq, K.; Sim, M.; Black, R.; Stack, M. Mapping the Micro-Abrasion Mechanisms of CoCrMo: Some Thoughts on Varying Ceramic Counterface Diameter on Transition Boundaries In Vitro. *Lubricants* **2020**, *8*, 71. [[CrossRef](#)]
15. El Hassanin, A.; Quaremba, G.; Sammartino, P.; Adamo, D.; Miniello, A.; Marenzi, G. Effect of Implant Surface Roughness and Macro- and Micro-Structural Composition on Wear and Metal Particles Released. *Materials* **2021**, *14*, 6800. [[CrossRef](#)] [[PubMed](#)]
16. Pu, J.; Wu, D.; Zhang, Y.; Zhang, X.; Jin, Z. An Experimental Study on the Fretting Corrosion Behaviours of Three Material Pairs at Modular Interfaces for Hip Joint Implants. *Lubricants* **2021**, *9*, 12. [[CrossRef](#)]
17. Buj-Corral, I.; Vidal, D.; Tejo-Otero, A.; Padilla, J.A.; Xuriguera, E.; Fenollosa-Artés, F. Characterization of 3D Printed Yttria-Stabilized Zirconia Parts for Use in Prostheses. *Nanomaterials* **2021**, *11*, 2942. [[CrossRef](#)] [[PubMed](#)]
18. Li, H.; Liu, X.; Zhang, C.; Jiao, X.; Chen, W.; Gao, J.; Zhong, L. Friction and Wear Properties of Silicon Nitride-Based Composites with Different HBN Content Sliding against Polyether-Etherketone at Different Speeds under Artificial Seawater Lubrication. *Coatings* **2022**, *12*, 411. [[CrossRef](#)]
19. Varanasi, D.; Furkó, M.; Balázsi, K.; Balázsi, C. Processing of Al<sub>2</sub>O<sub>3</sub>-AlN Ceramics and Their Structural, Mechanical, and Tribological Characterization. *Materials* **2021**, *14*, 6055. [[CrossRef](#)] [[PubMed](#)]
20. Carreiras, A.R.; Fonseca, E.M.M.; Martins, D.; Couto, R. The Axisymmetric Computational Study of a Femoral Component to Analysis the Effect of Titanium Alloy and Diameter Variation. *J. Comput. Appl. Mech.* **2020**, *51*, 403–410. [[CrossRef](#)]
21. Fernandes, M.G.; Alves, J.L.; Fonseca, E.M.M. Diaphyseal Femoral Fracture: 3D Biomodel and Intramedullary Nail Created by Additive Manufacturing. *Int. J. Mater. Eng. Innov.* **2016**, *7*, 130. [[CrossRef](#)]
22. Strømmen, E.N. *Structural Mechanics*; Springer International Publishing: Cham, Switzerland, 2020. [[CrossRef](#)]
23. Ammarullah, M.I.; Afif, I.Y.; Maula, M.I.; Winarni, T.I.; Tauviqirrahman, M.; Jamari, J. Tresca Stress Evaluation of Metal-on-UHMWPE Total Hip Arthroplasty during Peak Loading from Normal Walking Activity. *Mater. Today Proc.* **2022**, *63*, S143–S146. [[CrossRef](#)]
24. Ammarullah, M.I.; Afif, I.Y.; Maula, M.I.; Winarni, T.I.; Tauviqirrahman, M.; Bayuseno, A.P.; Basri, H.; Syahrom, A.; Saad, A.P.M.; Jamari, J. 2D Computational Tresca Stress Prediction of CoCrMo-on-UHMWPE Bearing of Total Hip Prosthesis Based on Body Mass Index. *Malaysian J. Med. Heal. Sci.* **2021**, *17* (Suppl. 13), 18–21.
25. Ammarullah, M.I.; Afif, I.Y.; Maula, M.I.; Winarni, T.I.; Tauviqirrahman, M.; Akbar, I.; Basri, H.; Van Der Heide, E.; Jamari, J. Tresca Stress Simulation of Metal-on-Metal Total Hip Arthroplasty during Normal Walking Activity. *Materials* **2021**, *14*, 7554. [[CrossRef](#)]
26. Jamari, J.; Ammarullah, M.I.; Saad, A.P.M.; Syahrom, A.; Uddin, M.; van der Heide, E.; Basri, H. The Effect of Bottom Profile Dimples on the Femoral Head on Wear in Metal-on-Metal Total Hip Arthroplasty. *J. Funct. Biomater.* **2021**, *12*, 38. [[CrossRef](#)] [[PubMed](#)]
27. Jin, Z.M.; Dowson, D.; Fisher, J. Fluid Film Lubrication in Natural Hip Joints. *Tribol. Ser.* **1993**, *25*, 545–555. [[CrossRef](#)]
28. Dubiel, A.; Grabowski, G.; Goły, M.; Skrzypek, S. The Influence of Thermal Residual Stresses on Mechanical Properties of Silicon Nitride-Based Composites. *Materials* **2020**, *13*, 1092. [[CrossRef](#)] [[PubMed](#)]
29. Aherwar, A.; Singh, A.K.; Patnaik, A. Current and Future Biocompatibility Aspects of Biomaterials for Hip Prosthesis. *AIMS Bioeng.* **2015**, *3*, 23–43. [[CrossRef](#)]
30. Uddin, M.S.; Zhang, L.C. Predicting the Wear of Hard-on-Hard Hip Joint Prostheses. *Wear* **2013**, *301*, 192–200. [[CrossRef](#)]
31. Jagatia, M.; Jin, Z.M. Elastohydrodynamic Lubrication Analysis of Metal-on-Metal Hip Prostheses under Steady State Entraining Motion. *Proc. Inst. Mech. Eng. Part H J. Eng. Med.* **2001**, *215*, 531–542. [[CrossRef](#)] [[PubMed](#)]
32. Shankar, S. Predicting Wear of Ceramic–Ceramic Hip Prosthesis Using Finite Element Method for Different Radial Clearances. *Tribol.-Mater. Surfaces Interfaces* **2014**, *8*, 194–200. [[CrossRef](#)]
33. Cilingir, A.C.; Ucar, V.; Kazan, R. Three-Dimensional Anatomic Finite Element Modelling of Hemi-Arthroplasty of Human Hip Joint. *Trends Biomater. Artif. Organs* **2007**, *21*, 63–72.
34. Banchet, V.; Fridrici, V.; Abry, J.C.; Kapsa, P. Wear and Friction Characterization of Materials for Hip Prosthesis. *Wear* **2007**, *263*, 1066–1071. [[CrossRef](#)]
35. D’Andrea, D.; Pistone, A.; Risitano, G.; Santonocito, D.; Scappaticci, L.; Alberti, F. Tribological Characterization of a Hip Prosthesis in Si<sub>3</sub>N<sub>4</sub>-TiN Ceramic Composite Made with Electrical Discharge Machining (EDM). *Procedia Struct. Integr.* **2021**, *33*, 469–481. [[CrossRef](#)]
36. Ruggiero, A.; D’Amato, R.; Sbordone, L.; Haro, F.B.; Lanza, A. Experimental Comparison on Dental BioTribological Pairs Zirconia/Zirconia and Zirconia/Natural Tooth by Using a Reciprocating Tribometer. *J. Med. Syst.* **2019**, *43*, 97. [[CrossRef](#)] [[PubMed](#)]
37. Shankar, S.; Nithyaprakash, R. Wear Prediction on Silicon Nitride Bearing Couple in Human Hip Prosthesis Using Finite Element Concepts. *Proc. Inst. Mech. Eng. Part J J. Eng. Tribol.* **2014**, *228*, 717–724. [[CrossRef](#)]
38. Radu, A.-F.; Bungau, S.G.; Tit, D.M.; Behl, T.; Uivaraseanu, B.; Marcu, M.F. Highlighting the Benefits of Rehabilitation Treatments in Hip Osteoarthritis. *Medicina* **2022**, *58*, 494. [[CrossRef](#)] [[PubMed](#)]
39. Jamari, J.; Ammarullah, M.I.; Santoso, G.; Sugiharto, S.; Supriyono, T.; van der Heide, E. In Silico Contact Pressure of Metal-on-Metal Total Hip Implant with Different Materials Subjected to Gait Loading. *Metals* **2022**, *12*, 1241. [[CrossRef](#)]
40. Dassault Systèmes. *ABAQUS Analysis User’s Guide Volume IV: Elements*; Dassault Systèmes: Vélizy-Villacoublay, France, 2016.

41. Jamari, J.; Ammarullah, M.I.; Santoso, G.; Sugiharto, S.; Supriyono, T.; Prakoso, A.T.; Basri, H.; van der Heide, E. Computational Contact Pressure Prediction of CoCrMo, SS 316L and Ti6Al4V Femoral Head against UHMWPE Acetabular Cup under Gait Cycle. *J. Funct. Biomater.* **2022**, *13*, 64. [[CrossRef](#)]
42. Tan, N.; van Arkel, R. Topology Optimisation for Compliant Hip Implant Design and Reduced Strain Shielding. *Materials* **2021**, *14*, 7184. [[CrossRef](#)]
43. Ammarullah, M.I.; Afif, I.Y.; Maula, M.I.; Winarni, T.I.; Tauviqirrahman, M.; Bayuseno, A.P.; Basri, H.; Syahrom, A.; Saad, A.P.M.; Jamari. Wear Analysis of Acetabular Cup on Metal-on-Metal Total Hip Arthroplasty with Dimple Addition Using Finite Element Method. *AIP Conf. Proc.* **2022**, *2391*, 020017. [[CrossRef](#)]
44. Kim, J.S.; Heng, L.; Chanchannan, S.; Mun, S.D. Machining the Surface of Orthopedic Stent Wire Using a Non-Toxic Abrasive Compound in a Magnetic Abrasive Finishing Process. *Appl. Sci.* **2021**, *11*, 7267. [[CrossRef](#)]
45. Gonzalez, R.; Muñoz-Mahamud, E.; Bori, G. One-Stage Hip Revision Arthroplasty Using Megaprosthesis in Severe Bone Loss of The Proximal Femur Due to Radiological Diffuse Osteomyelitis. *Trop. Med. Infect. Dis.* **2021**, *7*, 5. [[CrossRef](#)]
46. Falisi, G.; Foffo, G.; Severino, M.; Di Paolo, C.; Bianchi, S.; Bernardi, S.; Pietropaoli, D.; Rastelli, S.; Gatto, R.; Botticelli, G. SEM-EDX Analysis of Metal Particles Deposition from Surgical Burs after Implant Guided Surgery Procedures. *Coatings* **2022**, *12*, 240. [[CrossRef](#)]
47. Solarino, G.; Carlet, A.; Moretti, L.; Miolla, M.P.; Ottaviani, G.; Moretti, B. Clinical Results in Posterior-Stabilized Total Knee Arthroplasty with Cementless Tibial Component in Porous Tantalum: Comparison between Monoblock and Two Pegs vs. Modular and Three Pegs. *Prosthesis* **2022**, *4*, 160–168. [[CrossRef](#)]
48. Basri, H.; Syahrom, A.; Prakoso, A.T.; Wicaksono, D.; Amarullah, M.I.; Ramadhoni, T.S.; Nugraha, R.D. The Analysis of Dimple Geometry on Artificial Hip Joint to the Performance of Lubrication. *J. Phys. Conf. Ser.* **2019**, *1198*, 042012. [[CrossRef](#)]
49. Lee, H.K.; Kim, S.M.; Lim, H.S. Computational Wear Prediction of TKR with Flatback Deformity during Gait. *Appl. Sci.* **2022**, *12*, 3698. [[CrossRef](#)]
50. Świczko-Żurek, B.; Zieliński, A.; Bociaga, D.; Rosińska, K.; Gajowiec, G. Influence of Different Nanometals Implemented in PMMA Bone Cement on Biological and Mechanical Properties. *Nanomaterials* **2022**, *12*, 732. [[CrossRef](#)] [[PubMed](#)]